chem. Biophys. Acta 85, 322.
Golichowski, A., Harruff, R. C., and Jenkins, W. T. (1971), *Fed. Proc., Fed. Am. Soc. Exp. Biol. 30,* 1211.
Grisolia, S. S., and Burris, R. H. (1954), *J. Biol. Chem. 210.*
Harley-Mason, J. (1961), *Arch. Biochem. Biophys. 93,* 178.
Hilton, M. A., Bornes, F. W., Henry, S. S., and Enns, T. W. (1954), *J. Biol. Chem. 209,* 743.
Hilton, M. A., Bornes, F. W., Henry, S. S., and Enns, T. W. (1956), *J. Biol. Chem. 219,* 833.
Ivanov, V. I., and Karpeisky (1969), *Adv. Enzymol. 32,* 21.
Johnston, R. B., Scholz, J. J., Diven, W. F., and Shepherd, S. (1966), Second Symposium on Chemical and Biological Aspects of Pyridoxal Catalysis, Moscow, Sept, New York, N.Y., Interscience.
Manning, J. M., Merrifield, N. E., Jones, W. M., and Gotschlich, E. C. (1974), *Proc. Natl. Acad. Sci. U.S.A. 71,* 417.
Metzler, E. D., Ikawa, M., and Snell, E. E. (1954), *J. Am. Chem. Soc. 76,* 648.
Oshima, T., and Tamiya, N. (1959), *J. Biochem. (Tokyo) 46,* 1675.
Oshima, T., and Tamiya, N. (1961), *Biochem. J. 78,* 116.
Saier, M. H., Jr., and Jenkins, W. T. (1967), *J. Biol. Chem. 242,* 91, 101.
Walter, U., Luthe, H., Gerhart, F., and Sölung, H. (1975), *Eur. J. Biochem. 34,* 395.
Whelan, D. J., and Long, G. J. (1969), *Aust. J. Chem. 22,* 1779.

Intact Photoreceptor Membrane from Bovine Rod Outer Segment: Size and Shape in Bleached State†

Takashi Norisuye,‡ William F. Hoffman,§ and Hyuk Yu*

ABSTRACT: Photoreceptor disk membranes isolated from bovine rod outer segments are suspended in dilute aqueous sucrose (4.36×10^{-3}%) and bleached, and their size and shape are determined with quasielastic and elastic light scattering. They are found to be extremely homogeneous spherical vesicles with a radius of 0.49 ± 0.07 μm which appear to have derived from the native disk shape by osmotic swelling.

The visual process involves complex sequences of events in transducing photochemical energy to electrical energy (Wald, 1968; Rodieck, 1973; Kliger and Menger, 1975). A vast literature has accumulated delineating the role of the visual pigment membrane in this process (Hagins, 1972; Abrahamson, 1975). Our goal is to isolate disk membranes from vertebrate rod outer segments (ROS[1]) as intact as possible and focus on their static and dynamic structure vis-à-vis the photoreceptor function.

This report represents a preliminary step toward that end: namely, the characterization of photoreceptor membranes suspended in dilute aqueous sucrose. Their size and shape are determined from quasielastic and elastic light-scattering measurements.

Experimental Procedure

Material. Except for some minor changes, the procedure of Smith et al. (1975) was used for the isolation and purification of bovine ROS membranes. For each preparation, 2–3 g of frozen retinae (Hormel Co.) was thawed with stirring in 9 ml of 36% sucrose–buffer (0.068 M sodium phosphate buffer, pH 7) for 30 min at 4 °C. The resulting suspension was diluted to 18 ml with 36% sucrose–buffer, passed through a wide-gauge syringe needle two to three times to effect complete suspension, layered with 15 ml of buffer, and then centrifuged for 1 h at 25 000 rpm in an SW-27 rotor (Beckman, Model L5-50 centrifuge). The crude outer segments that floated to the sucrose–buffer interface were harvested with a syringe, suspended in buffer, and pelleted by centrifugation at 15 000 rpm for 20 min. The supernatant was decanted and the pellet was resuspended in 36% sucrose–buffer. The ROS were floated again, and the carpet (the material which collected at the sucrose–buffer interface) was divided into two parts for the second washing in buffer. Each of the purified pellets was gently rinsed with 5% aqueous Ficoll (molecular weight 400 000; Sigma) to minimize the amount of remaining buffer in the tube and finally suspended in 17 ml of 5% Ficoll. Dust-free nitrogen gas was bubbled through the Ficoll suspensions and they were left standing overnight in the dark at 4 °C to allow complete bursting of the rods. The ROS disk membranes were harvested from the surface of each Ficoll solution after centrifugation at 25 000 rpm for 2 h. All the above operations were performed under a dim red light (Kodak No. 1 filter, 15-W bulb) at 4 °C. To check the purity of the ROS disk membranes so obtained, the absorbances A_{498} at 498 nm and A_{278} at 278 nm were measured on a Gilford spectrophotometer. The ratios A_{278}/A_{498} were substantially constant (2.46 ± 0.23) for the five independent preparations (see below), indicating that our preparations were reasonably pure (Raubach et al., 1974a; Smith et al., 1975).

Quasielastic Light Scattering. The instrument, the data acquisition scheme, and the spectrum analysis method employed here have been described elsewhere (Shaya et al., 1974).

† From the Department of Chemistry, University of Wisconsin, Madison, Wisconsin 53706. *Received August 4, 1976.* Supported by National Institutes of Health Grant EY01483.

‡ On leave from the Department of Polymer Science, Osaka University, Toyonaka, Osaka, Japan.
§ Wisconsin Alumni Research Foundation fellow and National Science Foundation Predoctoral trainee.

[1] Abbreviations used: ROS, rod outer segment; QLS, quasielastic light scattering; ELS, elastic light scattering.

The homodyne beat technique (Cummins and Swinney, 1970) was adopted for the detection of the quasielastically scattered light; the incident light (He/Ne laser, 632.8-nm wavelength; Spectra-Physics 135) and scattered light are both vertically polarized. The measurements were made on three independently prepared samples at room temperature. The membranes, purified as described above, were suspended in 4.36×10^{-3}% aqueous sucrose, whose molar concentration is equivalent to 5% Ficoll, and the suspension was filtered through a 10-μm pore size Teflon filter (Millipore) directly into a light scattering cell. Subsequently, dust-free nitrogen gas was bubbled through the solution to retard oxidation of the membrane phospholipids and the cell was capped with a plastic stopper. Finally, the suspension was bleached by exposure to fluorescent lamps for 10–15 min.

For a dilute monodisperse system of spherical particles, the power spectrum $S(\nu)$ is given by (Cummins and Swinney, 1970; Pecora, 1972; Chu, 1974; Berne and Pecora, 1976):

$$S(\nu) = A\left[\frac{\Delta\nu_{1/2}}{\nu^2 + (\Delta\nu_{1/2})^2}\right] + B \qquad (1)$$

where A and B are constants representing respectively the integrated spectral intensity and the apparent shot noise, ν is the broadened frequency (from the incident frequency), and $\Delta\nu_{1/2}$ is the half-width at half-height of the single Lorentzian profile (the first term in the above equation). The half-width $\Delta\nu_{1/2}$ is related to the translational diffusion coefficient D by

$$\Delta\nu_{1/2} = \frac{D\kappa^2}{\pi} \qquad (2)$$

which is used to evaluate D from the slope of a plot of $\Delta\nu_{1/2}$ against κ^2/π. Here κ is the magnitude of the scattering wave vector defined as $(4\pi/\lambda')\sin(\theta/2)$ with the wavelength of the incident light in the scattering medium λ' and the scattering angle θ. We analyzed the data of the quasielastic light scattering (QLS) from the ROS membrane suspensions using eq 1 and 2. The analyses of the observed power spectra were effected via a nonlinear regression method on a UNIVAC 1110 computer. The regression routine provided the mean values and 95% confidence intervals of the three parameters, $\Delta\nu_{1/2}$, A, and B in eq 1.

Elastic Light Scattering. Elastic light scattering was performed on a SOFICA photogoniometer (Bausch and Lomb; Model 40000). The incident green light (546 nm) and scattered light were both vertically polarized, and the scattered intensity was monitored at 1° increments for an angular range of 30–150°. The background scattering correction was effected as follows. By taking advantage of the large size of the principal component (i.e., membranes), we removed it from the suspension by passing it through 0.22-μm Millipore filters two to three times and the resulting filtrate was regarded as contributing to the background. The scattered intensity of the filtrate was then subtracted from that of whole suspension. This converse procedure from the customary background correction was adopted because the optical clarification of the whole suspension was not readily performable due to the large size of the principal scattering component. Since two separately prepared samples were both diluted by 100-fold from the concentration employed in the QLS measurements, no attempt was made to examine the concentration dependence of the intensity profile.

Results and Discussion

Figure 1A illustrates a Doppler broadened power spectrum of the scattered light from an ROS membrane preparation in 4.36×10^{-3}% aqueous sucrose at an angle of 50°. Each solid curve (linear frequency scale on the bottom and logarithmic frequency scale on the top) is a single Lorentzian profile with a half-width at half-height $\Delta\nu_{1/2}$ of 16 Hz. In Figure 1B we display its normalized residuals plot; the deviations of the experimental points from the fitted Lorentzian profile are plotted against ν. The lack of systematic trends in the residuals indicates that the single Lorentzian profile adequately represents the experimental data. Similar results were obtained for different preparations and at different angles. The angular dependence of $\Delta\nu_{1/2}$ is displayed in Figure 1C, where $\Delta\nu_{1/2}$ is

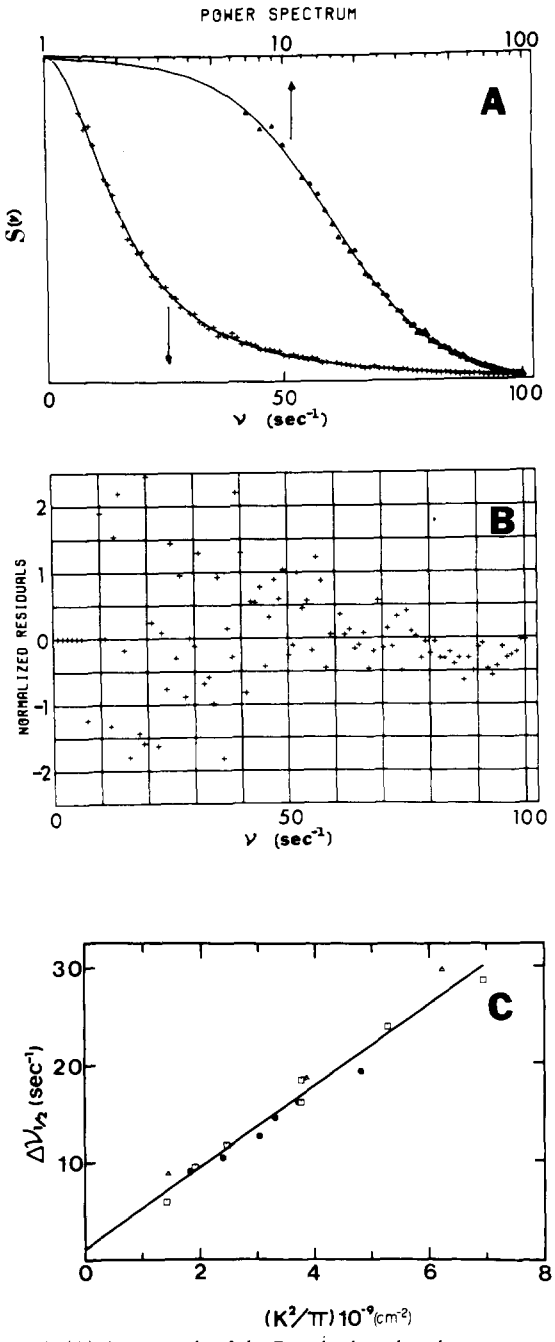

FIGURE 1: (A) An example of the Doppler broadened power spectrum of the scattered light from a photoreceptor membrane preparation at an angle of 50°. Each solid curve (lower abscissa; linear frequency scale; upper abscissa; logarithmic frequency scale) is a single Lorentzian profile with a half-width $\Delta\nu_{1/2}$ at half-height of 16 Hz. (B) The normalized residuals of A plotted against frequency ν. (C) Plots of $\Delta\nu_{1/2}$ vs. κ^2/π. Three independently prepared samples are distinguished by different symbols.

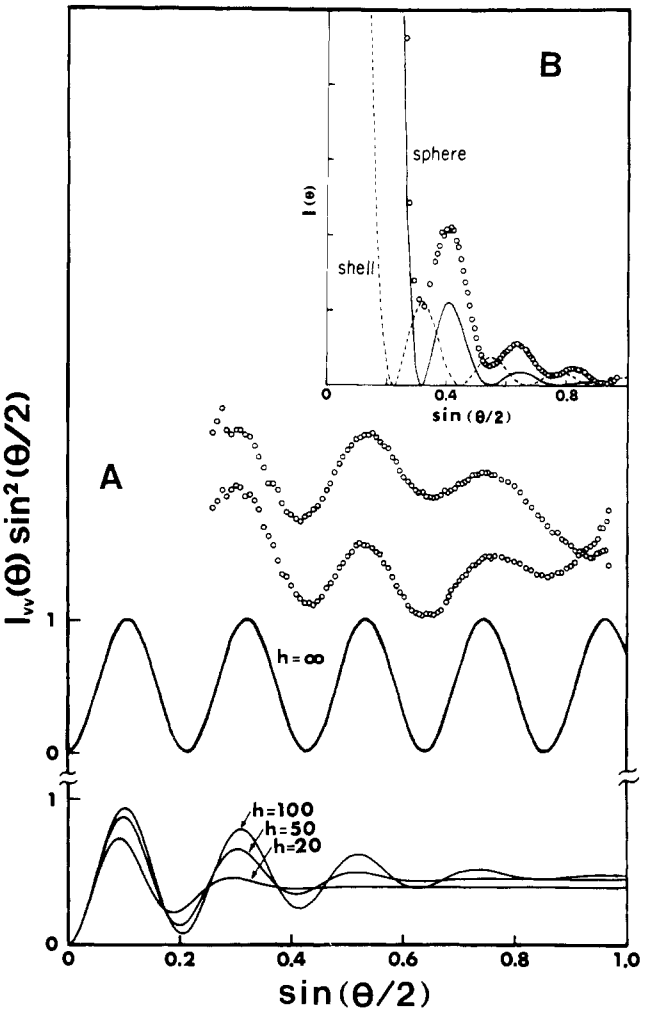

FIGURE 2: (A) The intensity modulation profiles of two independently prepared suspensions of the ROS membranes are displayed by plots of $I_{vv}(\theta)\sin^2(\theta/2)$. The two data sets (in arbitrary units) are deliberately shifted to exhibit the reproducibility of the maxima and minima whereas for the theoretical (solid) curves, $P(\kappa)(\kappa R_0)^2$ or $\langle P(\kappa)\rangle\ (\kappa\langle R_0\rangle_w)^2$ is plotted against $\sin(\theta/2)$. The parameters used for the calculation of the theoretical curves are: $R_0 = 0.48\ \mu m$ for monodisperse spherical shells ($h = \infty$) and $\langle R_0\rangle_w = 0.48\ \mu m$ for polydisperse spherical shells of the indicated h values. (B) Comparison of the intensity profiles of solid sphere (solid) and spherical shell (dashed) is given by two theoretical curves; the experimental data for polystyrene latex (0.45 μm radius) are represented by the circles. Here, the plot is $I(\theta)$ vs. $\sin(\theta/2)$ unlike those in A.

plotted against κ^2/π in accordance with eq 2. Here, three independently prepared samples are distinguished by different symbols. As expected, the plotted points follow the same straight line for each of the different preparations. A statistical analysis with 14 degrees of freedom (16 data points) with the aid of Student's t distribution (Draper and Smith, 1966) gives the slope and intercept as $(4.19 \pm 0.45) \times 10^{-9}$ cm^2/s and 1.17 ± 1.73 s^{-1}, respectively, within 95% confidence limits. Hence, the intercept can be taken to be zero within the experimental uncertainty which is in accord with eq 2. We therefore conclude that the experimental results from QLS are consistent with the monodisperse sphere model. From the value of $D = (4.19 \pm 0.45) \times 10^{-9}$ cm^2/s at 25 °C, we calculate a Stokes radius of $0.51 \pm 0.05\ \mu m$ using the Stokes–Einstein equation

$$D = \frac{kT}{6\pi\eta_0 R} \tag{3}$$

Here kT has the usual meaning and η_0 is the medium viscosity which was separately measured for each suspension.

We now turn to the results of the elastic light scattering (ELS) measurements. We shall present a brief discussion of the model to be chosen and then describe the results in terms of the model. If our ROS membranes are indeed single-bilayered vesicles in dilute aqueous sucrose and the intravesicular fluid contributes negligibly to the light scattering of the whole vesicles, then the observed particle scattering factor should conform to that of the hollow sphere model. Pecora and Aragón (1974) have derived the particle scattering factor of hollow spheres with membrane vesicles in mind. The hollow sphere model reduces to the simpler spherical shell model when the inner radius approaches the outer radius; since the bilayer thickness of the ROS membranes is small (~75 Å; Worthington, 1973) compared with the Stokes radius (5100 Å), we postulate that the ROS membranes may conform to the spherical shell model. The particle scattering factor of a spherical shell with optically isotropic scattering elements, all located on the surface of a sphere with the radius R_0, is given by (Oster and Riley, 1952)

$$P_i(\kappa R) = \left(\frac{\sin \kappa R_0}{\kappa R_0}\right)^2 \equiv [j_0(\kappa R_0)]^2 \tag{4}$$

where j_0 stands for the zero-order spherical Bessel function. When $\kappa R_0 \geq 1$, this equation gives a damped modulation profile for the particle scattering factor. Since the reciprocal scattering wave vector κ^{-1} in our ELS measurements is comparable to or less than the Stokes radius of the ROS membranes, the condition $\kappa R_0 \geq 1$ is fulfilled in this experiment and we should expect such a modulated profile if this model is in fact applicable. We note further that, under such a circumstance, the function $\kappa^2 P_i(\kappa R_0)$ oscillates with a constant amplitude; the extrema of these oscillations are determined by the condition $\kappa R_0 = n\pi/2$ where even integers of n represent the minima and odd integers the maxima. In case of optical isotropy or small anisotropy (see below) of the scattering elements, the polarized scattering intensity $I_{vv}(\theta)$ from dilute solution is directly proportional to the particle scattering factor Therefore, the intensity profile and the extrema positions with respect to the scattering angle should provide shape and size information about the membranes.

Since $\sin(\theta/2)$ and $I_{vv}(\theta)$ are respectively proportional to κ and $P_i(\kappa)$, a plot of $\sin^2(\theta/2)I_{vv}(\theta)$ vs. $\sin(\theta/2)$ is equivalent to a plot of $\kappa^2 P_i(\kappa)$ vs. κ. In Figure 2A, we display such a plot, where two sets of experimental data are given by unfilled circles and the theoretically predicted profile for monodisperse spherical shells with $R_0 = 0.48\ \mu m$ is shown by the solid curve drawn immediately below. General features of the experimental and theoretical profiles are in a good agreement, and a radius of $0.48 \pm 0.06\ \mu m$ is determined from the extrema positions. Hence, we conclude that the ROS membranes can successfully be represented by the spherical shell model which is in turn consistent with a single-bilayered membrane vesicle.

We now discuss two important points: the optical anisotropy of the scattering elements and the polydispersity of our samples. The polarized scattering factor for the spherical shell model, for the case of anisotropic scattering elements with cylindrical symmetry, may be expressed as (Pecora and Aragón, 1974)

$$P_{vv}(\kappa R_0) = C[P_i^{1/2}(\kappa R_0) + \gamma P_a^{1/2}(\kappa R_0)]^2 \tag{5}$$

where C is a normalization constant, $P_i(\kappa R_0)$ is the isotropic particle scattering factor given by eq 4, $P_a(\kappa R_0)$ is the anisotropic scattering factor which is identical with the squared

second-order spherical Bessel function $j^2(\kappa R_0)$, and γ is the optical anisotropy of a scattering element defined as $(\alpha_1 - \alpha_2)/(\alpha_1 + 2\alpha_2)$ with α_1 and α_2 referring respectively to the longitudinal and transverse components of the polarizability tensor in the scattering-element-fixed coordinate system. With the aid of eq 5, we address the question of whether a set of R_0 and γ can be determined uniquely. Values of R_0 were calculated from the extrema positions predicted by eq 5 at different values of γ. It was found that the values of R_0 were the same, within the experimental uncertainty, for $0 \leq |\gamma| \leq 0.25$, and that no other values of R_0 were consistent with the experimental data irrespective of γ values outside of this range. Thus the shell radius is uniquely determined within the range of the optical anisotropy of the scattering elements. Although no explicit measurement of γ has been made for the ROS disk membranes, it seems reasonable that the γ value should lie within this range.

Next, we attempt to extract a measure of the distribution of the vesicular radius from the experimental data. Since the power spectra fit quite well to a single Lorentzian profile, we suspect that the distribution of the vesicular radius is reasonably smooth and does not deviate substantially from the monodisperse limit. We therefore try to analyze the polydispersity in terms of a smooth distribution function. We adopt the Schulz–Zimm distribution function (Schulz, 1939; Zimm, 1948) for the purpose. It is described by two parameters: the first parameter, describing the breadth of the size distribution, is designated as h and the second parameter, representing a given mean size, is chosen here as the weight-average radius $\langle R_0 \rangle_w$ (a particular choice out of various mean quantities is immaterial, see Appendix). The monodisperse limit is given by $h = \infty$ and the limit of the most probable distribution by $h = 1$. We calculate the average particle scattering factor (expected to be sampled by the experiment) at different values of h with $\langle R_0 \rangle_w$ fixed at the value of R_0 deduced for $h = \infty$ (see Appendix). The predicted intensity profiles are drawn in solid curves in the bottom of Figure 2A. It is clear that the intensity modulation curve of $\kappa^2\langle P(\kappa) \rangle$ damps out more rapidly as the distribution is broadened, i.e., $h \to 1$. A comparison of the experimental data with the theoretical curves indicates that h must be larger than 100 to allow observation of three maxima and minima in the scattering angle range examined; otherwise, some or all of these features would be obscured by the damping of the particle scattering factor. For $h \geq 100$, the weight to number average ratio of the radii $\langle R_0 \rangle_w / \langle R_0 \rangle_n$ is less than 1.01 (given by eq A5 in the Appendix) which indicates an extremely narrow distribution of the vesicular radius. Having thus established a relative insensitivity of the R_0 determination on γ within a reasonable range and a rather narrow distribution of R_0 in our preparations, we conclude that ELS measurements confirm the shape of the ROS membranes to be vesicular and provide the size as 0.48 ± 0.06 μm in the radius.

Lastly, we shall discuss the experiment designed to answer a question of whether our ELS results can rule out the isotropic solid sphere model. The question is related to whether the intravesicular fluid in fact contributes negligibly to the light scattering of whole vesicles. For this purpose, we performed a scattering study of a similarly sized solid sphere particle of 0.45 μm in radius, a polystyrene latex (Dow). In this experiment we monitored the scattered intensity without the polarizer or analyzer. Thus the intensity is designated as $I(\theta)$ without the subscripts. The result is displayed in Figure 2B. The scattered intensity $I(\theta)$ is plotted against $\sin(\theta/2)$ and compared with the theoretical curves for an isotropic solid sphere (solid curve) and an isotropic spherical shell (dashed curve), both with a radius of 0.46 μm. Since the ordinate here is $I(\theta)$ instead of $\sin^2(\theta/2)I_{vv}(\theta)$ as in Figure 2A, the intensity profiles appear as damped sinusoids unlike those in Figure 2A where the damping has been suppressed in order to emphasize the extrema positions. The dashed curve (spherical shell) is obtained from eq 4 with $R_0 = 0.46$ μm and the solid curve from eq 5 with $\gamma = 1$ and $R_0 = 0.46$ μm; the solid curve is drawn according to the particle scattering factor for the isotropic solid sphere model which is the same as eq 5 with $\gamma = 1$ (Kerker, 1969). The experimental profile is in excellent agreement with the solid sphere model within the experimental uncertainty and qualitatively different from the spherical shell model. The data for the ROS membranes on the other hand are in agreement with the shell model when they are similarly plotted. Thus, we conclude that the solid sphere model can indeed be ruled out for the shape of the ROS disk membranes in this concentration of aqueous sucrose. This lends support to our earlier assumption that the intravesicular fluid contributes negligibly to the scattering.

We now make contact with other studies on the size and shape of the ROS disk membranes. The value of 0.98 ± 0.14 μm for the diameter (arithmetic mean of $2R$ from QLS and $2R_0$ from ELS) determined in this study is quite close to the value of 1 μm obtained from the freeze-fracture electron micrographs of bovine ROS disk membranes osmotically swollen in water (Raubach et al., 1974b). In addition, it has been shown that the diameter of the flattened disks in the rod outer segment is approximately 1.5 μm (McConnell, 1965). If the ROS disks swell osmotically with their surface area unchanged, then the diameter of the swollen membranes should be reduced by a factor of $2^{1/2}$ from that of the disk form as proposed by Raubach et al. (1974b); the values for the diameter determined by us and by Raubach et al. support this proposal. It is possible, however, that the photoreceptor membranes have a finite elastic constant whereby osmotic swelling might result in isotropic stretching of the vesicular surface depending on the osmolarity of the suspending medium. Under such a circumstance, the conclusion relative to the conservation of surface area of the native disk state must be moderated. Raubach et al. (1974b) have also found from the freeze-fracture experiments that the membranes osmotically swollen in water are roughly spherical and moderately homogeneous in their size distribution. Their findings substantially agree with our results from quasielastic and elastic light scattering. It is to be noted, however, that detailed determinations of the shape and size distribution of vesicles by electron microscopy are difficult because three-dimensional reconstruction is required from the two-dimensional projection of cross-sectioned spheres. Furthermore, electron microscopic examinations require either chemical fixation or freezing which might change the shape and size characteristics of the vesicles from those in solution. Our methods, on the other hand, extract the vesicular size and shape in a well-defined medium in situ.

In summary, two points should be noted: (1) the ratio of the weight to number average radii deduced from the intensity modulation profile is no larger than 1.01 on the basis of Schulz–Zimm distribution for the radius, indicating that the membranes are extremely homogeneous in size, and (2) the radius of 0.48 ± 0.06 μm from the ELS study is in accord with the Stokes radius of 0.51 ± 0.05 μm from the QLS study. The mean radius from the two methods is 0.49 ± 0.07 μm. We might add here that Chen et al. (1976) have recently shown that phosphatidylcholine vesicles can also be characterized as Stokes spheres by a QLS study. Since we have shown that the equilibrium vesicular radius is the same as the Stokes radius

from QLS, subsequent investigations involving the photochemical state of the membranes (bleached vs. unbleached) can be conducted by the QLS technique. The results will be reported in a forthcoming paper.

Acknowledgment

We are most grateful to Professor M. T. Record for his willing assistance including loan of some equipment. We thank Professor C. B. Kasper for advice and critical comments.

Appendix

We derive the particle scattering factor for a polydisperse system of spherical shells composed of optically isotropic scattering elements. The average particle scattering factor $\langle P(\kappa)\rangle$ is given by (Zimm, 1948):

$$\langle P(\kappa)\rangle = \frac{\sum_i n_i P_i(\kappa R_i) f_w(n_i)}{\sum_i n_i f_w(n_i)} \tag{A1a}$$

$$= \frac{\sum_i n_i^2 P_i(\kappa R_i) f_n(n_i)}{\sum_i n_i^2 f_n(n_i)} \tag{A1b}$$

where n_i is the number of scattering elements on the surface of the shells whose radius is R_i, $f_w(n_i)$, and $f_n(n_i)$ are, respectively, the weight and number fractions of the shells having n_i scattering elements, and $P_i(\kappa R_i)$ is the particle scattering factor of the shells with the radius R_i. Assuming that the distribution of $f_n(n_i)$ is smooth and continuous, we may replace the sum in eq A1b by an integral. Thus

$$\langle P(\kappa)\rangle = \frac{\int_0^\infty n^2 P(\kappa R) f_n(n)\mathrm{d}n}{\int_0^\infty n^2 f_n(n)\mathrm{d}n} \tag{A2}$$

With use of the relationship $f_n(n)\mathrm{d}n = f(R)\mathrm{d}R$ and the proportionality of n to the surface area $4\pi R^2$, eq A2 is rewritten as

$$\langle P(\kappa)\rangle = \frac{\int_0^\infty R^4 P(\kappa R) f_n(R)\mathrm{d}R}{\int_0^\infty R^4 f_n(R)\mathrm{d}R} \tag{A3}$$

where $f_n(R)$ is the number fraction of shells having a radius in the range of R and $R + \mathrm{d}R$. In order to evaluate the above integral, an explicit expression for $f_n(R)$ is needed. We use the Schulz–Zimm distribution function (Schulz, 1939; Zimm, 1948)

$$f_n(R) = \frac{1}{h!}\left[\frac{h+1}{\langle R_0\rangle_w}\right]^{h+1} R^h \exp\left[-\frac{(h+1)R}{\langle R_0\rangle_w}\right] \tag{A4}$$

because of its mathematical tractability and a broad applicability to polydisperse systems (Zimm, 1948; Benbasat and Bloomfield, 1972; Aragon and Pecora, 1976). The weight-average radius $\langle R_0\rangle_w$ is related to the other average radii in the Schulz–Zimm distribution by

$$\frac{h}{\langle R_0\rangle_n} = \frac{h+1}{\langle R_0\rangle_w} = \frac{h+2}{\langle R_0\rangle_z} \tag{A5}$$

where $\langle R_0\rangle_n$ and $\langle R_0\rangle_z$ are the number average and the z-average radii, respectively. Finally, substitution of $P(\kappa R) = [j_0(\kappa R)]^2$ and eq A4 into A3, followed by integration, yields

$$\langle P(\kappa)\rangle = \frac{(h+1)^2}{2(h+3)(h+4)} \frac{1}{[\langle R_0\rangle_w \kappa]^2} \times \left\{1 - \left[1 + \left(\frac{2\langle R_0\rangle_w \kappa}{h+1}\right)^2\right]^{-(h+3)/2} \times \cos\left[(h+3)\arctan\left(\frac{2\langle R_0\rangle_w \kappa}{h+1}\right)\right]\right\} \tag{A6}$$

In the limit of $h = \infty$, eq A6 reduces to eq 4 for monodisperse spherical shells. The curves in the bottom of Figure 2A are drawn according to eq A6 with $\langle R_0\rangle_w = 0.48$ μm with different values of h as indicated in the figure.

References

Abrahamson, E. W. (1975), *Acc. Chem. Res. 8,* 101.
Aragón, S. R., and Pecora, R. (1976), *J. Chem. Phys. 64,* 2395.
Benbasat, J. A., and Bloomfield, V. A. (1972), *J. Polym. Sci., Polym. Phys. Ed. 10,* 2475.
Berne, B. J., and Pecora, R. (1976), Dynamic Light Scattering, New York, N.Y., Wiley.
Chen, F. C., Chrzeszczyk, A., and Chu, B. (1976), *J. Chem. Phys. 64,* 3403.
Chu, B. (1974), Laser Light Scattering, New York, N.Y., Academic Press.
Cummins, H. Z., and Swinney, H. L. (1970), *Prog. Opt. 8,* 133.
Draper, N. R., and Smith, H. (1966), Applied Regression Analysis, New York, N.Y., Wiley.
Hagins, W. A. (1972), *Annu. Rev. Biophys. Bioeng. 1,* 131.
Kerker, M. (1969), The Scattering of Light, New York, N.Y., Academic Press.
Kliger, D. S., and Menger, E. L. (1975), *Acc. Chem. Res. 8,* 81.
McConnell, D. G. (1965), *J. Cell Biol. 27,* 459.
Oster, G., and Riley, D. P. (1952), *Acta Crystallogr. 5,* 1.
Pecora, R. (1972), *Annu. Rev. Biophys. Bioeng. 1,* 257.
Pecora, R., and Aragón, S. R. (1974), *Chem. Phys. Lipids 13,* 1.
Raubach, R. A., Franklin, L. K., and Dratz, E. A. (1974a), *Vision Res. 14,* 335.
Raubach, R. A., Nemes, P. P., and Dratz, E. A. (1974b), *Exp. Eye Res. 18,* 1.
Rodieck, R. (1973), in The Vertebrate Retina, San Francisco, Calif., W. H. Freeman.
Schulz, G. V. (1939), *Z. Phys. Chem. B 43,* 25.
Shaya, S. A., Han, C. C.-C., and Yu, H. (1974), *Rev. Sci. Instrum. 45,* 280.
Smith, H. G., Jr., Stubbs, G. W., and Litman, B. J. (1975), *Exp. Eye Res. 20,* 211.
Wald, G. (1968), *Science 162,* 230.
Worthington, C. R. (1973), *Exp. Eye Res. 17,* 487.
Zimm, B. H. (1948), *J. Chem. Phys. 16,* 1099.